LUNAR SOUTH POLE MINERAL MAP PRODUCTS FROM KAGUYA MULTIBAND IMAGER. J. J. Blalock[1], D. P. Mayer[1], M. Lemelin[2], L. Sun[3], P. G. Lucey[3], L. R. Gaddis[1], and T. M. Hare[1]. [1]United States Geological Survey, Astrogeology Science Center, Flagstaff, AZ, USA; [2]Département de Géomatique appliquée, Université de Sherbrooke, Sherbrooke, Québec, Canada; [3]Hawaii Institute of Geophysics and Planetology, Department of Geology and Geophysics, University of Hawaii at Manoa, Honolulu, HI, USA.

Introduction: We present new lunar south pole mineral map products derived from images captured by the Kaguya Multiband Imager (MI). Kaguya MI captures images in 5 visible (VIS) spectral channels (415, 750, 900, 950, and 1001 nm) and 4 near-infrared (NIR) spectral channels (1000, 1050, 1250, and 1550 nm) [1]. From a nominal orbital altitude of 100 km, VIS images have a spatial resolution of 20 m per pixel and NIR images have a spatial resolution of 62 m per pixel [2]. Below we describe the development of south polar modeled mineral abundance maps of olivine, orthopyroxene, clinopyroxene, plagioclase, FeO, and submicroscopic metallic iron (SMFe). We also provide south polar maps of optical maturity (OMAT), the plagioclase grain size, and the weighted criteria calculated to identify the best spectral match between each MI spectrum and a spectral library. Here we discuss the procedure for creating the mineral map products and our recent efforts to produce higher resolution versions of these map products and making them all available at 20 m per pixel.

Datasets: New derived mineral maps were created using MI reflectance data from Version 3 of the Japanese Space Agency's (JAXA's) MAP Level 2 processing. At this processing level, reflectance measurements have been converted to 1°x1° mosaics and map-projected into a simple cylindrical frame. Additionally, the reflectances have been corrected to account for effects of topographic shading and normalized to a standard viewing geometry as described by Ohtake et al. [3]. These data are available online from the Kaguya (SELENE) data archive at: http://l2db.selene.darts.isas.jaxa.jp/index.html.en.

Global Maps: The first step in our reprocessing was to generate global cylindrically-projected mineral maps. Mineral map data were derived using the same procedure and algorithms as those previously presented by Lemelin et al. [4,5,6]. Nearly global lunar coverage is achieved, except for missing MI frames. The result of this process is 64,202 individual 1°x1° raster tiles that contain 9 bands, one band for each of the derived minerals and modeled products described above. Each raster tile has a spatial resolution of ~60 m per pixel, is ~10 MB in volume, and has an associated detached ENVI-style geospatial header.

After creating the raster tiles, they are mosaicked together in a 2-step process to create the cylindrically-projected mineral map products. For each of the 9 mineral products, the associated band from each raster tile is first extracted and added into a GDAL Virtual Format Header (VRT) mosaic file. This results in 9 VRT mosaics that are ~32 MB in volume, one for each of the mineral products. These VRT mosaics are then converted into uncompressed GeoTIFFs with associated detached ISIS3 labels. Each of these final mosaics has a spatial resolution of ~60 m per pixel and is ~68 GB in volume. After mosaicking, each GeoTIFF is given a PDS4 compliant detached label.

Mineral map products were processed using the USGS Astrogeology Center computing cluster, with 2 weeks of computing time necessary to fully process the map products [7]. These products will be made available in PDS4 compliant format at the USGS Annex website at: https://astrogeology.usgs.gov/pds/annex.

Polar Maps: The global cylindrically-projected map products were then re-projected into a polar stereographic projection to produce the south pole mineral maps we present here (***Figure 1***). The maps are centered on the south pole (90°S) and extend out to 70°S, with a resolution of 60 m per pixel. Although MI data gaps and effects from illumination geometry and shadowing result in a lower signal-to-noise ratio than at the equatorial and mid-latitudes, these derived mineral maps still reveal useful information about the presence and distribution of several minerals in the south polar region. For example, the FeO map (***Figure 1d***) clearly highlights the mafic volcanic deposits within Schrödinger crater (75ºS, 132ºE; bottom right) and the ejecta surrounding De Forest crater (77ºS, 162ºW; bottom left). At a distance of ~450 km from the south pole, the Schrödinger crater volcanics may provide the closest point to sample the primitive mafic materials and possible resources (iron, oxygen) associated with such deposits [e.g., 8].

Higher Resolution Products: We are also working to produce versions with a spatial resolution of ~20 m per pixel (at native resolution for the VIS bands, upsampled for the NIR bands); these represent a considerable spatial improvement over currently available lunar mineral map products. These higher resolution products will be substantially larger than the ~60 m per pixel versions described here, with each final mosaic approaching ~1 TB in volume and requiring several weeks of computer processing time. Therefore, careful thought must be given to how best to make these products available for the community while maintaining their scientific

usefulness. We are currently exploring map tiling schemes to both maintain fidelity of the mineral maps at the improved spatial resolution and usability for users who wish to download and work with the products. Resampled, intermediate spatial resolution versions may also be produced if warranted. The new, higher resolution products will also be delivered in PDS4 formats via the Annex of the PDS Cartography and Imaging Sciences Node.

References: [1] Ohtake, M. et al. (2008) *EPS*, *60*, 257-264. [2] Haruyama, J. et al. (2008) *EPS*, *60*, 243-255. [3] Ohtake, M. et al. (2008) *Icarus*, *226*, 364-374. [4] Lemelin, M. et al. (2016) *47th LPSC*, abs. 2994.[5] Lemelin, M. et al. (2015) *JGR*, *120*, 869-887. [6] Lemelin, M. et al. (2019) *Planet. And Space Sci.*, *165*, 230-243. [7] Blalock, J. et al. (2020) *51st LPSC*, in press. [8] Shearer, C. et al., this volume.

Acknowledgments: This work was supported by the NASA Planetary Data Archiving, Restoration, and Tools (PDART) grant NNX17AK92G (P.G. Lucey, PI).

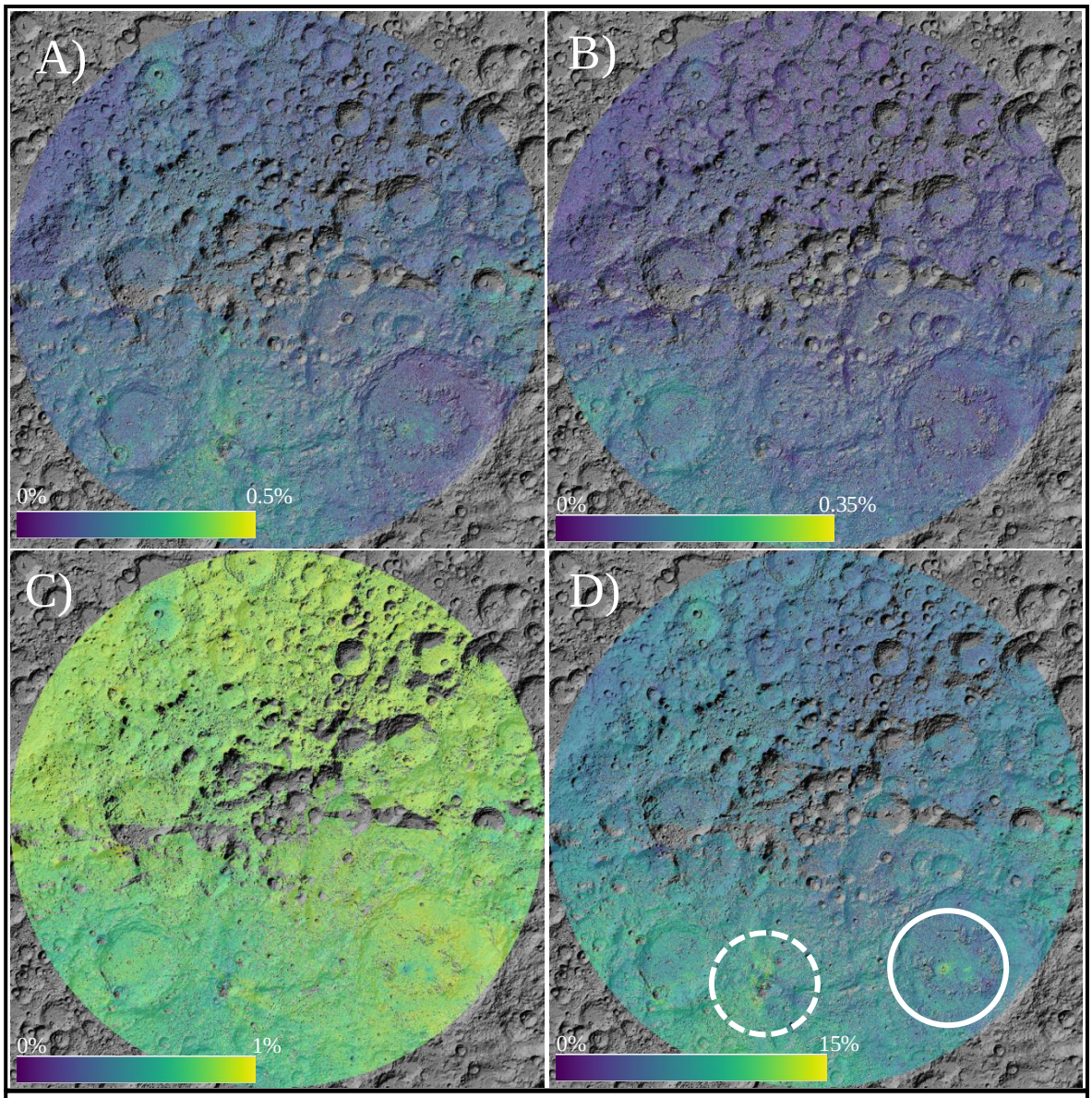

Figure 1. South polar mineral maps produced using the Kaguya Multiband Imager data: A) low-calcium pyroxene abundance (weight %), B) clinopyroxene abundance (weight %), C) plagioclase abundance (weight %), D) FeO abundance (weight %). Solid circle highlights mafic deposits in Schrödinger crater. Dashed circle highlights the ejecta around De Forest crater.